Tuning the absorptions of Au nanospheres on a microshell by photo-deformation

2006 Nanotechnology 17 4600

(http://iopscience.iop.org/0957-4484/17/18/012)

INSTITUTE OF PHYSICS PUBLISHING NANOTECHNOLOGY
Nanotechnology **17** (2006) 4600–4605 doi:10.1088/0957-4484/17/18/012

Tuning the absorptions of Au nanospheres on a microshell by photo-deformation

Li-Hsin Han[1,2], **Tingji Tang**[2,3] **and Shaochen Chen**[1,2,4]

[1] Department of Mechanical Engineering, University of Texas at Austin, Austin, TX 78712, USA
[2] Center for Nano- and Molecular Science and Technology, University of Texas at Austin, Austin, TX 78712, USA
[3] Department of Chemistry and Biochemistry, University of Texas at Austin, Austin, TX 78712, USA

E-mail: scchen@mail.utexas.edu

Received 19 May 2006, in final form 27 July 2006
Published 29 August 2006
Online at stacks.iop.org/Nano/17/4600

Abstract
We report the design, modelling, fabrication, and testing of a photo-tunable particulate medium that comprises photo-responsible polymeric microshells covered by Au nanospheres. The microshells were formed by a layer-by-layer method. The charged Au nanospheres were coated on outer surfaces of the microshells. The polymeric shells contain azobenzene moieties and shrink upon ultraviolet irradiation; therefore, the interparticle spaces between the nanospheres are tunable by UV light. The absorption spectrum of the Au nanosphere modified microshells changed drastically after the shrinkage. A decreased absorption peak of Au nanospheres and an enhanced absorption in the near-infrared region were clearly observed. The results of theoretical modelling suggest that the overall spectral changes stem mainly from the enhanced particle interactions and also from the field enhancements in the space among the nanospheres.

M Supplementary data files are available from stacks.iop.org/Nano/17/4600

1. Introduction

The optical interactions among small particles under irradiation have become attractive topics for more than a century [1–6]. The particle interactions include surface plasmon coupling and interparticle field enhancement. These interactions, which are originally from the multiple scattering of light by individual particles [1], depend strongly on the spacing among neighbouring particles. The particle interactions become significant when the particle spacing is small compared to the wavelength of incident light [2]. A particulate medium (a medium that comprises small particles) with small particle spacing may present very different optical properties from that of the individual particles [1, 2]. Recent technology advancement allows one to use nanometre scale patterns to demonstrate the effects of changing the interparticle spacing on the absorption of light [2, 3]. The effects observed include the shifting and dividing of absorption peaks, and the increase of absorption in a certain spectral range. These studies have shed light on the possibility of developing a particulate medium of desirable optical properties by choosing specific particles and by controlling the interparticle spacing; the studies also provide intuitive concepts applicable to many fields, including photochemistry reagents, optical communication media, and passive optical devices [4–6].

Optically induced deformation of polymers containing azobenzene (AZO) moieties has attracted considerable attention in recent years [7–10]. Through *trans*-to-*cis*-state isomerization induced by ultraviolet (UV) light, an azobenzene molecule changes its molecule length (from approximately 9.0 to 5.5 Å), space occupation, and polarity [7]. These changes could induce length reduction and molecule migration [8, 9], which enable AZO-polymers to directly convert photons to mechanical energy and generate observable deformation in the polymer matrix. Important applications of AZO-polymers include photo-bending of AZO-polymeric thin films for microdevices [8], surface relief gratings (SRGs) for maskless microgroove formation, and SRG surfaces that record the

[4] Author to whom any correspondence should be addressed.

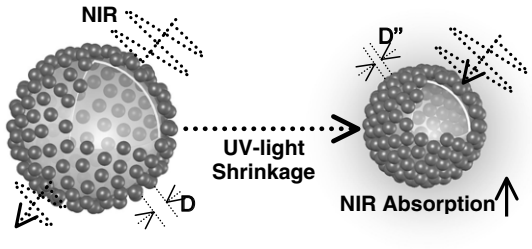

Figure 1. The illustration of a nanosphere-coated microshell tuned by UV light.

enhancement patterns of surface plasmons (also known as the near-field effect) [9]. The photo-isomerization effect was further applied to produce ellipsoidal submicron particles by irradiating spherical azobenzene micelles with polarized UV light [10].

Based on these studies about the small-particle interactions and the photo-isomerization of azobenzene moieties, we developed nanosphere-coated microshells that present tunability in particle spacings. Gold nanospheres of 40 nm diameter were coated on the microshells which comprise functional azobenzene groups. The microshells shrink upon the irradiation of UV light, and this shrinkage is followed by the changing of the particle spaces among the nanospheres. Figure 1 shows an illustration of the microshell. In our previous study [11], we have successfully employed polyelectrolytes that comprise azobenzene molecules to build the photo-deformable microshells using a layer-by-layer (LBL) method [12], which is a self-assembly technique used to construct thin films of tunable chemical and compositional properties. These microshells present significant contractions under the irradiation of UV light; in our testing, the maximum shrinkage of the microshells' diameter was about 40%, corresponding to a volume change of 78%. It has been shown that photo-deformation can be generated by the *trans*-to-*cis* photo-isomerization of the azobenzene moieties; however, other possible causes of our results, such as thermal effect and photo-induced cross-linking in the polyelectrolytes, should be investigated as well.

2. Experiments

2.1. Experiment setup

In this work, the suspension of the microshells was loaded into a quartz cuvette mounted on a UV–vis spectroscope (HP 8453) to detect the absorption spectrum. UV light (about 2 W cm^{-2} in intensity) from a UV lamp (Green Spot UV Source, 200 W) passed through the sample from the top of the cuvette. The absorption spectra of the microshells were recorded at different irradiation intervals. Sample drops were taken from the cuvette during the UV irradiation and were observed both by an optical microscope (Axiotron, Carl Zeiss, magnification: 50× to 1000×) in an aqueous environment and by a scanning-electrical microscope (SEM, LEO 1530) in a dehydrated state. An integrated CCD camera (CV-S3200CE, JAI Corporation) was used to capture the microscope images. The experiment was carried out at room temperature.

2.2. Preparation of microshells

The polyelectrolytes, poly (1,4,3 carboxy-4-hydroxyphenyl-azobenzenesulfonaide-1,-ethanediyl, sodium salt) (PAZO, polyanion, MW 65 000–100 000), poly-allylamine hydrochloride (PAH, polycation, MW ∼ 70 000), and poly (ethyleneimine) (PEI, polycation, MW ∼ 25 000), were purchased from Sigma-Aldrich (St Louis, USA). Silica microspheres (diameter = 5.66 μm) were purchased from Bangs' Laboratory (Fishers, USA). Gold nanospheres (40 nm in diameter, negatively charged on the surface by carboxylic groups) were purchased from British Biocell International (UK). All materials were used as received. The polyelectrolytes were dissolved in deionized (DI) water at 2 mg ml^{-1}. The pH values of PAZO, PAH, and PEI were about 7.0, 7.0, and 9.0, respectively. No other chemicals were added into the solution. The chemical structures of PAZO, PAH, and PEI are shown in figure 2(a).

Silica microspheres were used as templates for the microshell formation. To enhance the surface charge, the microspheres, which are negatively charged by hydroxyl groups (–OH), were pre-coated with PEI. 0.1 ml of SiO_2 microspheres (approximately 7×10^8 particles) were mixed into 14 ml of PEI solution. Then, the solution was stirred for 30 min to allow the PEI to coat the microspheres; this was followed by centrifuging and rinsing with DI water. Following the PEI coating, five additional layers of PAZO and PAH were alternatively coated onto the microspheres through similar procedures. The positively charged microspheres were then mixed into 14 ml of the negatively charged gold-nanosphere solution (concentration: approximately 1×10^{11} particles ml^{-1}). The solution was gently stirred for 1 h to allow the gold nanospheres to coat onto the microspheres. The solution was then rinsed and centrifuged at 3000 rpm. This coating procedure was repeated five times. The microspheres were then coated with a final layer of PAH to immobilize the Au nanospheres as expected. Following the coatings, the silica cores of the microspheres were etched away to form microshells by using 1:20 buffered hydrofluoride (BHF) for 30 min. The microshells were rinsed seven times to remove the excess BHF and fluoride products. Following all the above procedures except the coating of nanospheres, another group of microshells were made with only the polymeric film. These unmodified microshells were used for the control experiments.

Figure 2(b) shows an image of the as-formed microshells under the optical microscope. In an aqueous environment, the microshells (approximately 6.2 μm in diameter) were spherical and swollen. An SEM picture of a dehydrated microshell is shown in figure 2(c). In addition, figure 2(d) shows an SEM picture of microspheres before the core removal. The bright dots in the picture are the Au nanospheres. According to the SEM pictures, the number of nanospheres covering one microshell is about 14 000. This number was used for our simulation.

3. Results and discussion

3.1. Effects of UV irradiation

The experimental results showed that the UV irradiation deforms both the Au-coated group and the control group (no

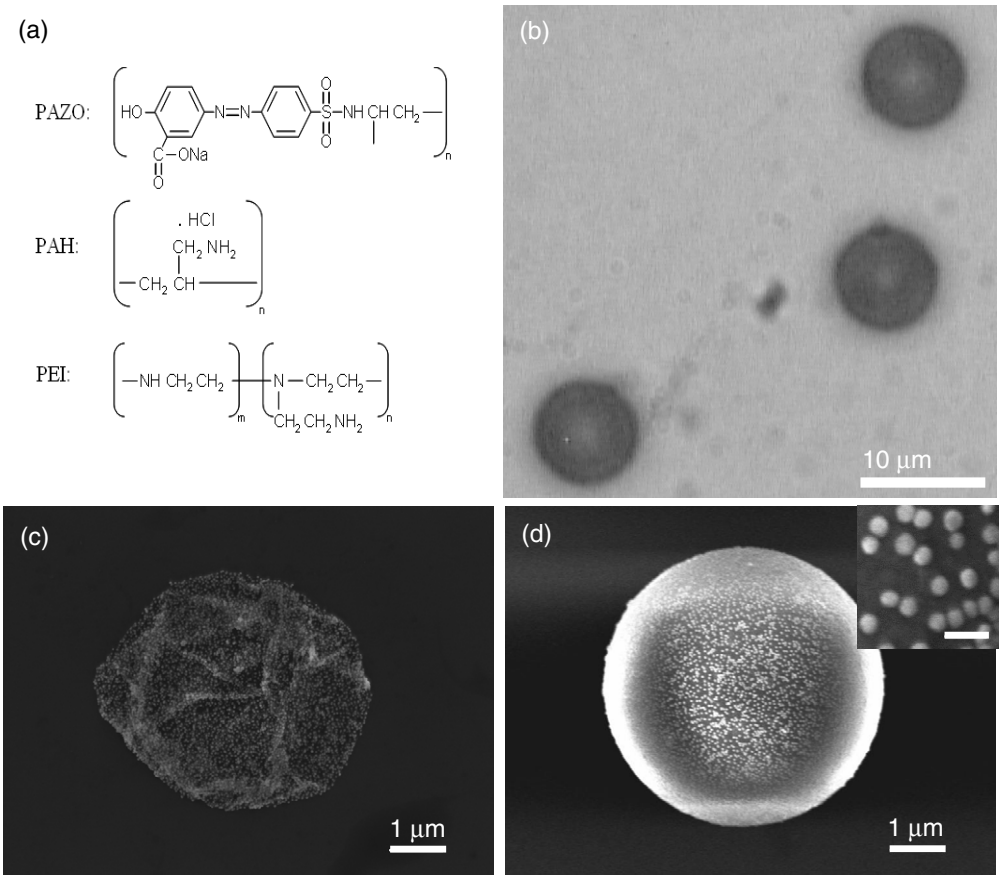

Figure 2. The Au-coated microshell: (a) the structures of the polyelectrolytes for building the microshells; (b) Au-coated microshells suspended in water; (c) an SEM picture of a dehydrated Au-coated microshell; (d) an SEM picture of an Au-coated microshell before the removal of the silica core. The inset in (d) shows the details on the surface; the bar indicates 100 nm.

Au nanospheres) of the microshells. The diameters of Au-coated microshell changed from 6.2 μm to about 4.0 μm in 14 min, as shown in figures 3(a) and (b). A similar result was obtained from the irradiation of the control group; the diameters of the irradiated polymeric microshells shrank about 40% before becoming stable.

Figure 3(c) shows the changes of absorption spectra of the Au-coated microshells (concentration: approximately 3×10^6 microshells ml^{-1}). The absorption spectra of the control microshells (approximately 2×10^7 microshells ml^{-1}) and that of diluted Au nanospheres (approximately 9×10^9 particles ml^{-1}) are shown in figures 3(d) and (e), respectively. The absorption peaks of the control microshells and the nanospheres were observed in the spectrum of the Au-coated microshells before irradiation. The UV-induced shrinkage considerably changed the absorption spectrum of the Au-coated microshells. Figure 3(c) showed a gradual rise in the near-infrared region (NIR) and a drop in the region around 560 nm, which is from the absorption peak (∼530 nm) of individual gold nanospheres. We also observed a significant decrease of the absorption in the UV region from 250 to 400 nm. The spectrum of the control group under the same irradiation and similar shrinkages showed non-obvious drops in the UV region and a minor rise in the NIR region (figure 3(d)), compared with those of the Au-loaded group.

Moreover, we observed a drastically enhanced absorption at a peak around 970 nm, as shown in figure 3(c). The location of the 970 nm peak matches the second-overtone band of water in the NIR [13]; the 970 nm peak before the UV irradiation might originate from the interaction between water and the concentrated polyelectrolytes in the microshells. Before the UV irradiation, this peak was weak but observable at the spectra of both groups. After the UV irradiation, the peak increases by more than tenfold in 14 min (see figure 3(c)).

3.2. Theoretical model

To study the mechanism behind the experimental results, we developed a theoretical model to simulate the interaction among the nanospheres. Our model is based on Mie's scattering theory [1] and the multipole approximation of dipole radiation [14–16].

Figure 4 illustrates our model that includes a monolayer of N nanospheres (of radius a and permittivity ε) on a large sphere of changing radius R. Each nanosphere generates a dipole moment $\vec{p}_m$ ($m = 1, 2, \ldots, N$) under the influence of an oscillating electric field $\vec{E}_{\rm inc}$ (if a sphere is sufficiently small compared to the wavelength λ of an incident light, its photo-reaction can be approximated with a dipole) [14]. $\vec{E}_{\rm inc}$ is polarized in the z-direction and vibrates with an angular frequency ω. The medium surrounding the dipoles has a

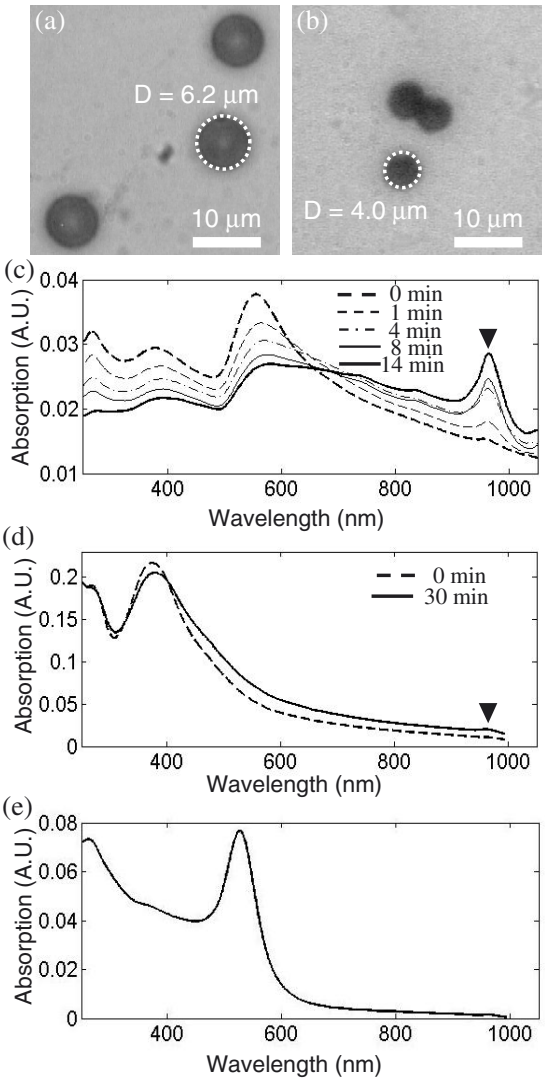

Figure 3. Experimental results of UV irradiation: (a) the microshells before irradiation; (b) the microshells after irradiation; the shell diameters reduced from 6.2 to 4.0 μm; (c) the change in the absorption spectrum of the Au-coated microshells at different intervals of irradiation; (d) the change in the absorption spectrum of the control group (microshells without Au); the peak around 370 nm is from the azobenzene group in the shells; (e) the absorption spectrum of diluted Au nanospheres. The arrows in (c) and (d) indicate an absorption peak observed at 970 nm.

permittivity of ε_m. The initial positions of the nanospheres $\vec{r}_{m0}$ $(m = 1, 2, \ldots, N)$ were randomly assigned. We also simulated the redistribution and aggregation of the nanospheres during the shrinkage of the microshell. As the radius of the large sphere changes to R from an initial value of R_0, the position of a nanosphere changes to $\vec{r}_m$ from the initial value of $\vec{r}_{m0}$. The value of $\vec{r}_m$ is numerically calculated based on Hooke's Law. In the model, it is assumed that the medium holds the nanospheres with a spring constant k_m, that the nanospheres in touch repel each other with a spring constant k_s, and that $k_s \gg k_m$. The dipoles in the model are given by [14]

$$\vec{p} = 4\pi\varepsilon_m a^3 \frac{\varepsilon_s - \varepsilon_m}{\varepsilon_s + 2\varepsilon_m}\vec{E}_{\text{inc}}. \tag{1}$$

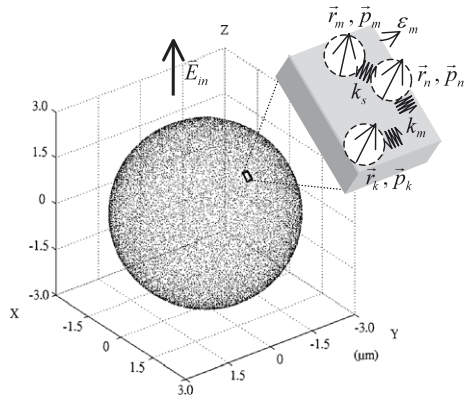

Figure 4. The theoretical model of a microshell: the positions $\vec{r}_m$ of the nanospheres on the microshell are randomly assigned; the values of polarization $\vec{p}_m$ (induced by $\vec{E}_{\text{in}}$) are calculated based on the theory of particle interactions; spring constants k_s and k_m are used to model the redistribution of nanospheres during the shrinkage of the microshell.

This approximate dipole has resonant modes with respect to the incident wavelength [15]. Absorption peaks are normally observed at these resonant modes and become the typical differences between the absorption spectrum of a small sphere and the spectrum of its parent bulk material. A comparison between the absorption of Au nanoparticles and an Au thin film has been studied [15b].

The approximate dipoles at different spheres may interact with each other. In the near zone ($|\vec{r}| \ll \lambda$), the electric field generated by a dipole at the origin point to a position $\vec{r}$ is given by [16]

$$\vec{E}(\vec{r}) = \frac{3(\vec{p}\cdot\hat{r})\hat{r} - \vec{p}}{4\pi\varepsilon_m|\vec{r}|^3}, \qquad \hat{r} = \vec{r}/|\vec{r}|. \tag{2}$$

When two spheres are very close, $\vec{E}_{\text{inc}}$ in equation (1) is dominated by $\vec{E}(\vec{r})$ from the neighbouring sphere; the approximate dipole of one sphere affects that of its neighbour and vice versa.

The photo-reaction of the nanospheres is calculated with different sets of $\vec{r}_m$ with respect to different values of R. According to equation (2), a dipole $\vec{p}_m$ affects the centre of the sphere n by an electric field $\vec{E}_{mn}$:

$$\vec{E}_{mn} = \frac{3(\vec{p}_m\cdot\hat{r}_{mn})\hat{r}_{mn} - \vec{p}_m}{4\pi\varepsilon_m r_{mn}^3}, \qquad r_{mn} = |\vec{r}_n - \vec{r}_m|. \tag{3}$$

The nanospheres have finite sizes; to consider the average effect of $\vec{p}_m$ onto the sphere n, we replace r_{mn} with an average value $\bar{r}_{mn}$, where

$$\bar{r}_{mn} = \left(\frac{1}{2a}\int_{r_{mn}-a}^{r_{mn}+a} r^{-3}\mathrm{d}r\right)^{-1/3}. \tag{4}$$

The electric field at dipole $\vec{p}_n$ is

$$\vec{E}_{\text{total},n} = \vec{E}_{\text{inc}} + \sum_{k=1(k\neq n)}^{N} \vec{E}_{kn}. \tag{5}$$

Combining equations (1), (3), and (5) gives

$$\vec{p}_n = \varepsilon_m \alpha \vec{E}_{\text{inc}} + \frac{\alpha}{4\pi} \sum_{k=1(k\neq n)}^{N} (3(\vec{p}_k \cdot \hat{r}_{kn})\hat{r}_{kn} - \vec{p}_k) \cdot |\vec{r}_{kn}|^{-3} \tag{6}$$

where $\alpha = 4\pi a^3(\varepsilon - \varepsilon_m)/(\varepsilon + 2\varepsilon_m)$. Using the Lorentz model [17], we calculated the total absorption W_{abs} by all nanospheres in the system:

$$W_{\text{abs}} = \sum_{m=1}^{N} \frac{\omega}{2} \text{Im}(\vec{p}_m \cdot \vec{E}^*_{\text{total},m}). \tag{7}$$

To simulate the field enhancement by the nanospheres, the electric field energy storage W_{store} inside the microshell was numerically calculated through an integration of the electric energy density over an interparticle-space volume υ, which covers the space from $r = R + a$ to $r = R - a$ excluding the nanosphere volume.

$$W_{\text{store}} = \int_{\upsilon} \tfrac{1}{4}\varepsilon_m (\vec{E}_{\text{inc}} + \vec{E}_{\text{s}}(\vec{r})) \cdot (\vec{E}_{\text{inc}} + \vec{E}_{\text{s}}(\vec{r}))^* \, \text{d}\upsilon \tag{8}$$

where $\vec{E}_{\text{s}}(\vec{r})$ is the electric field from all the nanospheres following equation (2). The values of ε, which are wavelength dependent, were taken from the literature [18]. The dimension constants in our model (R_0, N, and a) are from our measured data. The value of ε_m was assigned as 2.5, referring to literature [3a].

3.3. Comparison between the experimental and theoretical results

We used the results of our theoretical model to explain the changes of the modified microshell spectra in our experiment. Figure 5(a) shows the simulated absorption spectra of the gold nanospheres in different deformation stages. The simulated spectra show drops of the absorption peak around 530 nm and a drastic increase in NIR absorption; similar changes were observed in the experimental spectra as depicted in figure 3(c). Figure 5(b) shows the distribution of interparticle distances among neighbouring nanospheres; the number of particles in contact (at which $|r_{mn}| = 40$ nm) gradually increases as the shell radius shrinks. Note that, from equation (2), the particle interaction increases when the interparticle distance decreases. Therefore, the simulated spectra show that an overall decrease of the interparticle distance enhances the particle interaction and changes the nanosphere absorptions, including the drop around 530 nm and the rise in the NIR region.

The simulation results in figure 5(a) only include the absorption change of the Au nanospheres; the polymeric material was assumed to be non-absorptive (by using a real dielectric constant ε_m) in our model. Therefore, the result in figure 5(a) does not show the observed changes (figure 3(c)) at 970 nm and the UV region, which indicate the absorption changes of the polymeric material. The spectrum changes at 970 nm and the UV region, however, are explained by using the calculation of the energy storage W_{store}.

The absorption of electromagnetic energy by an optical system is proportional to the amount of energy stored in the system [17]. Accordingly, we may study the absorption changes at 970 nm and the UV region by using the

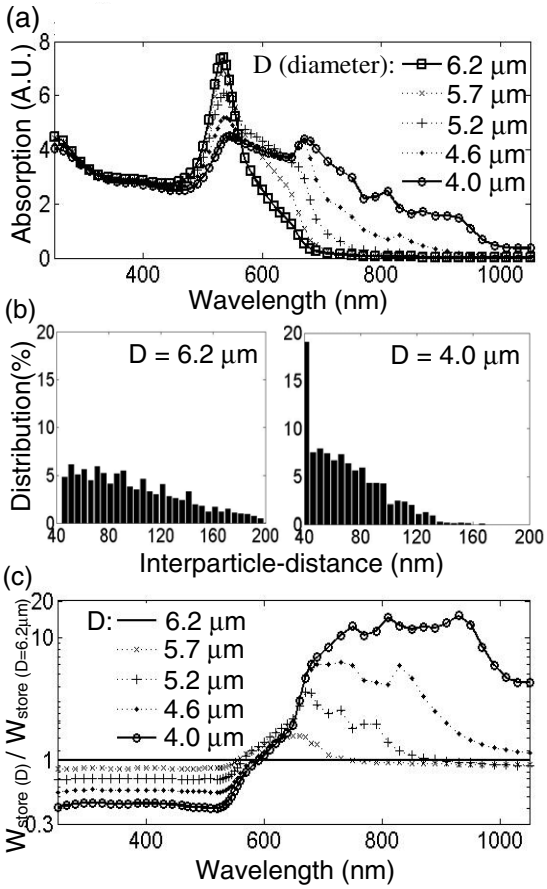

Figure 5. Simulation results of the microshell model (in which the microshell deforms from 6.2 to 4.0 μm): (a) the change in the absorption spectrum of the Au-coated microshells at different moments of deformation; (b) the change in the length distribution of the interparticle distances among neighbouring nanospheres; (c) the change of energy storage during the shrinkage; the effect of sphere shrinkage (D decrease) on the field enhancement is shown by the ratio $W_{\text{store}(D)}/W_{\text{store}(6.2\ \mu\text{m})}$. 6.2 μm is the initial shell diameter.

calculated value of W_{store}, which shows the energy storage in the polymeric material of the microshell (equation (8)). Figure 5(c) shows that W_{store} increases in the NIR region and decreases in the UV region as the shell diameter changes from 6.2 to 4.0 μm. In the NIR region, as the shell shrinks, the value of W_{store} increases by more than tenfold its initial value. This change indicates a significant field enhancement in the NIR region; the decrease of particle spacings aids the resonance of NIR electromagnetic wave. In the UV region, our calculation shows that the drop of W_{store} is due to the shell-volume decrease and also due to the lack of field enhancement in the UV region. The simulation results of W_{store} suggest that the increased absorption at the 970 nm peak and the absorption drop of the UV region in the experiment spectrum are due to the different degrees of field enhancement in the NIR and UV regions by the microshell, and also due to the volume contraction during the UV irradiation.

3.4. Recoverability of the UV-induced shrinkage

In theory, photo-isomerization of azobenzene can be recovered by keeping the sample in darkness (for several days) or upon

exposure to visible light [7]. We tested the recoverability of the photo-deformed microshells by irradiation using a laser with a visible wavelength (vis) (532 nm pulse laser, 10 mJ cm^{-2} per pulse, 10 Hz) and by using a white-light source. In our testing, however, the microshells did not present observable diameter recovery after the vis irradiation after 2 h; we only observed swellings in the thickness of the deformed microshell after the vis irradiation. The UV-processed microshells still retained their deformed diameters after a month in a dark environment. To date, the mechanism behind this non-recoverability remains unclear. Possible explanations include: (a) during the photo-induced contraction, the azobenzene moieties experienced a molecule migration, a phenomenon reported elsewhere [9]; (b) after the deformation, newly formed electrostatic attraction between the oppositely charged polyelectrolytes stabilized the deformed matrix. The geometric recoverability of the microshell could be realized by using a different kind of photo-sensitive polymer; see [8a] and [8b]. Supplementary material is available at stacks.iop.org/Nano/17/4600.

4. Conclusions

We have successfully developed a photo-tunable particulate medium, of which the NIR absorption is tunable by UV light. By using the LBL method with azobenzene-based polyelectrolytes, we fabricated gold-nanosphere-coated microshells that shrink upon UV irradiation. The shrinkage of the microshells reduces the interparticle spacing among nanospheres and causes drastic changes in the absorption spectrum and significantly enhanced absorption in the NIR region was observed. A comparison between our experiment and simulated results suggests: (a) the main cause of the spectrum changes was the enhancement of particle interactions among nanospheres, and (b) the UV-light-induced shrinkage significantly increases the nanosphere absorption and the field enhancement in the NIR region. This study has shed light on the applications of medium with photo-tunable functions, including biological diagnostics, photo-voltaic materials, and photo-catalysis reagents.

Acknowledgments

This work was partially supported by grants from the US National Science Foundation and Office of Naval Research. We thank Professor Stephen E Webber in the Department of Chemistry and Biochemistry at UT-Austin for equipment support.

References

[1] Mie G 1908 Beiträge zur Optik trüber Medien speziell kolloidaler Metallösungen *Ann. Phys.* **25** 376–445
[2] Tolga Atay T, Song J and Nurmikko A V 2004 *Nano Lett.* **4** 1627–31
Tamaru H, Kuwata H, Miyazaki H T and Miyano K 2002 *Appl. Phys. Lett.* **80** 1826
[3a] Schmitt J, Mächtle P, Eck D, Möhwald H and Helm C A 1999 *Langmuir* **15** 3256–66
[3b] Rechberger W, Hohenau A, Leitner A, Krenn J R, Lamprecht B and Aussenegg F R 2003 *Opt. Commun.* **220** 137–41
[4] Tian Y and Tatsuma T 2005 *J. Am. Chem. Soc.* **127** 7632–7
[5] Nomura W, Ohtsu M and Yatsui T 2005 *Appl. Phys. Lett.* **86** 181108
[6] Joannnopoulos J D, Meade R D and Winn J N 1995 *Photonic Crystal: Molding the Flow of Light* (Princeton, NJ: Princeton University Press)
[7] Feringa B L 2001 *Molecular Switches* (Weinheim: Wiley–VCH) p 399
[8a] Yu Y, Nakano M and Ikeda T 2003 *Nature* **425** 145
[8b] Ikeda T, Nakano M, Yu Y, Tsutsumi O and Kanazawa A 2003 *Adv. Mater.* **15** 201
[8c] Li M, Keller P, Li B, Wang X and Brunet M 2003 *Adv. Mater.* **15** 569
[9] Chung D, Fukuda T, Takanishi Y, Ishikawa K, Matsuda H, Takezoe H and Osipov M A 2002 *J. Appl. Phys.* **92** 1841
Bachelot R *et al* 2003 *J. Appl. Phys.* **94** 2060
[10] Li Y, He Y, Tong X and Wang X 2005 *J. Am. Chem. Soc.* **127** 2402
[11] Han L, Tang T, Chen S and Webber S E 2005 *Int. Conf. on Bio-Nano-Information Fusion (LA, USA)*
[12a] Decher G, Hong J D and Schmitt J 1992 *Thin Solid Films* **210** 831
[12b] Decher G 1997 *Science* **277** 1232
[12c] Caruso F 2000 *Chem. Eur. J.* **6** 413
[12d] Sukhorukov G B, Shchukin D G, Dong W, Möhwald H, Lulevich V V and Vinogradova O I 2004 *Macromol. Chem. Phys.* **205** 530
[12e] Schneider G and Decher G 2004 *Nano Lett.* **4** 1833
[12f] Mayya K S, Gittins D I, Dibaj A M and Caruso F 2001 *Nano Lett.* **1** 727
[13] Palmer K F and Williams D 1974 *J. Opt. Soc. Am.* **64** 1107–10
[14] Craig F B and Donld R H 1983 *Absorption and Scattering of Light by Small Particles* (Chichester: Wiley) pp 136–9
[15a] Craig F B and Donld R H 1983 *Absorption and Scattering of Light by Small Particles* (Chichester: Wiley) pp 325–9
[15b] Maier S A and Atwater H A 2005 *Appl. Phys. Rev.* **98** 011101
[16] Jackson J D 1999 *Classical Electrodynamics* 3rd edn (New York: Wiley) pp 407–11
[17] Jackson J D 1999 *Classical Electrodynamics* 3rd edn (New York: Wiley) pp 309–13
[18] Johnson P B and Christy R W 1972 *Phys. Rev.* B **6** 4370–9